The biochemical sensor based on liquid-core photonic crystal fiber filled with gold, silver and aluminum

Qiang Liu[a,b,*], Zhuang Ma[a], Qiang Wu[b], and Weilin Wang[a]

[a]*State Key Laboratory of Synthetical Automation for Process Industries, School of Control Engineering, Northeastern University at Qinhuangdao, Qinhuangdao, 066004, People's Republic of China*

[b]*Faculty of Engineering and Environment, Northumbria University, Newcastle Upon Tyne, NE1 8ST, United Kingdom*

*Corresponding author.
E-mail address: liuqiang@neuq.edu.cn (Q. Liu).

Abstract:

A highly sensitive SPR-PCF based biochemical sensor has been proposed based on finite element method simulations. Two metal wires are assumed to fill into two air holes in the y direction and the liquid analyte with refractive index higher than background material is injected into the central air hole. The liquid analyte supports liquid-core mode which couples to SPP mode as the phase matching condition is satisfied. High sensitivity of fiber sensor is achieved by the direct interaction between transmitted light and liquid analyte. The fiber sensor possesses the sensitivities of -8383.9 nm/RIU, -8428.6 nm/RIU and –8776.8 nm/RIU by filling gold, silver and aluminium respectively into the air holes of the PCF as the refractive index of liquid analyte varies from 1.454 to 1.478. The influences of the structural parameters of the PCF on the resonance wavelength and confinement loss are also analyzed.

Keywords: Surface plasmon resonance; Photonic crystal fiber; Biochemical sensor; Finite element method.

1. Introduction

Photonic crystal fibers (PCFs) are of significantly potential due to the periodic arrangement of air holes on its cross section which go through the whole fiber along the direction of light propagation [1]. Compared with conventional optical fibers, PCF

possesses many distinctive characteristics, such as flexible structural design, large mode area, high birefringence and low confinement loss [2], [3], [4], [5], [6], [7]. In recent years, PCFs have been broadly put into sensing fields because air holes existed provides a platform to integrate fiber and functional materials. Typical fiber materials are usually a bit sensitive to environment, it has been shown that the sensitivity of fiber sensors can be improved by filling sensitive materials into air holes of PCF [8], [9], [10]. In 1950s, R. H. Ritchie introduced surface plasmons theoretically for the first time [11]. Since then the surface plasmon resonance (SPR) technology has been gradually applied to the fiber devices [12], [13], [14]. The coupling resonance occurs between fiber mode and surface plasmon polariton (SPP) mode when the phase matching condition is satisfied by filling or coating plasma materials into air holes or on the fiber surface. H. W. Lee et al. proposed a novel fiber-splicing technique to pump molten gold into the air holes of PCF and a hollow channel of modified step index fiber, meanwhile dips were observed at the resonance wavelength in the transmission spectra [15]. Shuyan Zhang et al. studied the novel characteristics of metal-filled dual-core PCF based on supermode theory and coupled-mode theory, and found the coupling length between the two cores was reduced by the coupling resonance between core mode and SPP mode [16].

Chemical sensor is a device that can respond to chemical component in a small, specific and reversible way, and can produce a measurable signal proportional to the corresponding concentration. Biosensor is a highly selective monitor which uses the biological active units (such as enzyme, antibody, nucleic acid, cell, etc.) as the biological sensitive units. Because of the close relationship between chemical sensor and biosensor, they are often called biochemical sensors. The measurement of chemical refractive index is an important part of biochemical sensor. The maximum confinement loss appears at the resonance wavelength which is greatly sensitive to ambient variety and can be used to detect biochemical samples. Md. Rabiul Hasan et al. originally proposed a refractive index sensor employing niobium nanofilm and aluminum oxide (Al_2O_3) film coated on the PCF surface, which possesses the sensitivities of 3000 and 8000 nm/RIU at the refractive indices of 1.36, 1.40 respectively and the average sensitivity is just 5143 nm/RIU [17]. Ahmmed A. Rifat

et al. coated copper and graphene layer on the surface of PCF and made the sensor simpler practically with the sensitivity of 2000 nm/RIU in the detected range of 1.33-1.37 [18]. Zhenkai Fan et al. discussed the sensing characteristics of PCF with metal film coated on the surface of two air holes and the fiber sensor possesses the average sensitivity of 7017 nm/RIU as refractive index of analyte varies from 1.40 to 1.42 [19]. Zipeng Guo et al. realized a wide-range refractive index sensor based on PCF coated with gold film selectively and the sensitivity is -1931.03 nm/RIU in the refractive index range 1.35-1.46 [20]. Tianshu Li et al. studied H-Shaped PCF based refractive index sensor with the sensitivity of 2770 nm/RIU as the refractive index of analyte varies from 1.33 to 1.36 [21]. Meanwhile, many biochemical sensors based on D-shaped PCF coated with metal film have been proposed with high sensitivities [22], [23], [24], [25], [26], [27]. While the metal film on the surface of fiber or air holes is easy to fall off, and it is also easily oxidized, therefore the fiber sensors are not stable [17], [18], [19], [20], [21], [22], [23], [24], [25], [26], [27]. Fiber sensors based on PCF filled with metal wire are more stable compared with the structures described above, while the fiber sensors reported possess low sensitivity. Xujun Xin et al. proposed a gold-filled PCF sensor and the average refractive index sensitivity is only -4125 nm/RIU in the sensing range of 1.45-1.49 [28]. Nan Chen et al. utilized the dual-optofluidic-channel PCF filled with gold wire to realize a refractive index sensor with low sensitivity of 5500 nm/RIU [29]. Therefore, realizing a highly sensitive sensor is significant by filling metal wire into the air holes of PCF.

A SPR based biochemical sensor has been proposed based on metal-wire filled PCF whose core is made up of liquid analyte. The sensitivity of fiber sensor can be improved by the direct interaction between transmitted light and liquid analyte. The influences of gold, silver and aluminum on the sensing characteristics were analyzed. We also discussed the effects of structural parameters of PCF on the resonance wavelength and confinement loss. The fiber sensor possesses the high sensitivities of -8383.9 nm/RIU, -8428.6 nm/RIU and -8776.8 nm/RIU based on the PCF filled with gold, silver and aluminum respectively as the refractive index of liquid analyte varies from 1.454 to 1.478.

2. PCF structure and material parameters

The cross section of polarization-maintaining PCF filled with metal wire and high-index liquid analyte is shown in Fig. 1. The air holes are distributed on the cross section in triangular lattice whose lattice pitch is Λ=2 μm. The diameter of the green hole filled with liquid analyte is D_1=1.8 μm which supports liquid-core mode. The two yellow holes possess the diameter of D_2=1.2 μm which are assumed to be filled with metal wires. The bigger white holes possess the diameter of D_3=2.0 μm and the diameter of other air holes are represented by d=0.8 μm whose refractive index is 1.0. As a radiation absorber, the boundary condition of perfectly matched layer (PML) is used to fully absorb radiation energy in the outer region and can prevent the light from reflecting to interfere fiber mode.

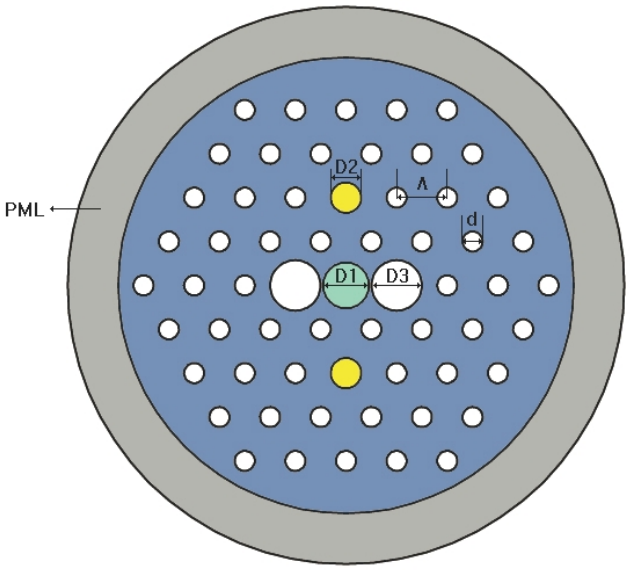

Fig. 1. Cross section of the proposed PCF filled with high-index liquid analyte in the central hole. The yellow holes are filled with metal wires.

The background material of PCF is fused silica whose wavelength-dependent refractive index is calculated by Sellmeier equation [30], and the ambient temperature T is assumed to be 25 ℃. The permittivity of gold wire is determined by Drude-Lorentz model [31]:

$$\varepsilon_m = \varepsilon_\infty - \frac{\omega_D^2}{\omega(\omega - j\gamma_D)} - \frac{\Delta\varepsilon \cdot \Omega_L^2}{(\omega^2 - \Omega_L^2) - j\Gamma_L\omega} \quad (1)$$

where ε_∞=5.9673 is the permittivity of gold in high frequency, $\Delta\varepsilon$=1.09 can be regarded as a weighting factor. ω_D is the plasma frequency and γ_D is the damping

frequency, where $\omega_D/2\pi$=2.113.6 THz, $\gamma_D/2\pi$=15.92 THz, ω is the angular frequency of transmitting light, Ω_L and Γ_L represent the frequency and the spectral width of the lorentz oscillator. Furthermore, $\Omega_L/2\pi$=650.07 THz, and $\Gamma_L/2\pi$=104.86 Hz. The permittivity of silver and aluminum can be expressed by Lorentz-Drude model [32]:

$$\varepsilon_r(\omega) = 1 - \frac{\Omega_p^2}{\omega(\omega - i\Gamma_0)} + \sum_{j=1}^{m} \frac{f_j \omega_p^2}{(\omega_j^2 - \omega^2) + i\omega\Gamma_j} \quad (2)$$

where ω_p is plasma frequency, m is oscillator number related to frequency ω_j, strength f_j and lifetime $1/\Gamma_j$; Ω_p is plasma frequency related to oscillator strength f_0 and damping constant Γ_0. The parameter values of silver and aluminum in Lorentz-Drude model are shown in Table Ⅰ and Table Ⅱ. The fabrication methods of PCF perform include ultrasonic drilling, cast rod in tube, extrusion, and stacking. Meanwhile, the drawing technology of PCF is very mature. Laser drilling method can be utilized to fill metal into PCF selectively [33]. Firstly, PCF and single-mode fiber are fused together. Then, femtosecond laser is used to drill holes on one end of the single-mode fiber making the holes interlinked with two holes of PCF to be filled. Last, molten metal can be filled into PCF selectively. The method can also be utilized for reference to fill liquid analyte into PCF selectively. Two ends of PCF are spliced with two sections of single-mode fiber. Femtosecond laser is used to drill two holes on the ends of the single-mode fibers respectively and the holes are interlinked with the central hole of PCF to be filled. One end of the combined fiber is put into syringe, the other end is put into liquid analyte, then the liquid analyte will be filled into the central hole of PCF by pressure of syringe. Light in spatial optical path can be used and it is easy to change liquid analyte to be detected.

Table Ⅰ: Parameter values of silver in Lorentz-Drude model

Parameters	ω_p	m	f_0	Γ_0	f_1	Γ_1	ω_1
Values	9.01	5	0.845	0.048	0.065	3.886	0.816
Parameters	f_2	Γ_2	ω_2	f_3	Γ_3	ω_3	f_4
Values	0.124	0.452	4.481	0.011	0.065	8.185	0.840
parameters	Γ_4	ω_4	f_5	Γ_5	ω_5		
Values	0.916	9.083	5.646	2.419	20.29		

Table Ⅱ: Parameter values of aluminum in Lorentz-Drude model

Parameters	ω_p	m	f_0	Γ_0	f_1	Γ_1	ω_1
Values	14.98	4	0.523	0.047	0.227	0.333	0.162
Parameters	f_2	Γ_2	ω_2	f_3	Γ_3	ω_3	f_4
Values	0.050	0.312	1.544	0.166	1.351	1.808	0.030
parameters	Γ_4	ω_4					
Values	3.382	3.473					

In this paper, the coupling between liquid-core mode and second-order surface plasmon polariton (SPP) mode is analyzed. The performances of SPR-fiber sensor are based on the confinement losse of liquid-core mode which can be defined by:

$$\alpha(x,y) = 8.686 \times \frac{2\pi}{\lambda} \mathrm{Im}(n_{eff}) \times 10^6 \quad (3)$$

where λ represents operating wavelength in μm, $\mathrm{Im}(n_{eff})$ is the imaginary part of effective refractive index of liquid-core mode, and the unit of mode loss is dB/m.

3. Results and discussion

Figure 2 shows the real parts of effective refractive index of core mode and SPP mode, and the loss of liquid-core mode dependence on wavelength in y-polarized direction. The plasma material is gold wire. The structural parameters are D_1=1.8 μm, D_2=1.2 μm, D_3=2.0 μm, d=0.8 μm, and Λ=2 μm. The maximum confinement loss appears at the resonance wavelength of 1367 nm as the refractive index of liquid analyte in the central hole is n_{eff}=1.458. The measurement range of refractive indices of liquid analyte is from 1.454 to 1.478 which is higher than the refractive index of fiber cladding, therefore the light can be guided in the core by total internal reflection. It can be found that the refractive indices of liquid-core mode and SPP mode decrease as wavelength increases, the liquid-core mode and SPP mode couple to each other strongest at one point which is the resonant wavelength and then transform into opponent mode respectively which means the liquid-core mode transforms into SPP mode and SPP mode transforms into liquid-core mode. For the black and upper curve,

the energy is mainly distributed in the gold-wire region at the shorter wavelengths and gradually transfers to the liquid-core region as wavelength increases. Moreover, almost the whole energy is distributed in the gold-wire region at the shorter wavelengths and in the liquid-core region at the longer wavelengths. The refractive indices of liquid-core mode and SPP mode are closest at the turning points of the curves which indicates the SPR occurs. The mode transition for the lower curve is just contrary to that for the upper curve. This is called complete coupling. Incomplete coupling has been introduced in [34], just a little energy of core mode couples to SPP mode at the resonance wavelength, and there is no transition between the two modes.

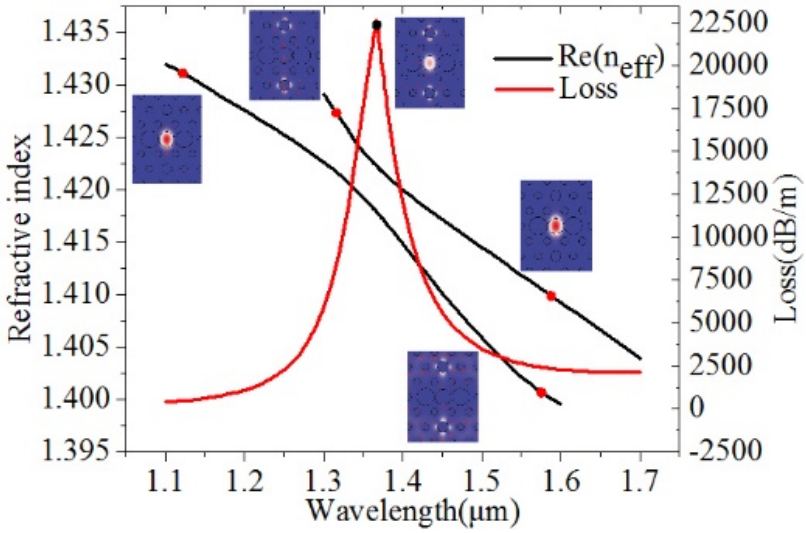

Fig. 2. Real parts of effective refractive index of liquid-core mode and SPP mode, and the confinement loss of liquid-core mode in y-polarized direction as the refractive index of liquid analyte is 1.458. The corresponding resonance wavelength is 1367 nm.

It is easy to know that fiber mode will be affected by the liquid analyte deeply due to that the fiber core consists of liquid analyte. Any tiny change of refractive index of liquid analyte will influence and lead to massive shift of resonance wavelength. In the simulation, we vary the refractive index of liquid analyte from 1.454 to 1.478 and the relation between confinement loss and wavelength is shown in Fig. 3. It can be seen intuitively that the resonance wavelength blue shifts as the refractive index of liquid analyte increases. Because the refractive index of liquid-core mode increases as the refractive index of liquid analyte increases, while that of SPP

mode is nearly not changed which leads the resonance point to short wavelength. Meanwhile, it is clearly seen that the confinement losse increases with the refractive index of liquid analyte increasing. According to the resonance wavelength, we plot a fitting line which is relative to corresponding refractive index of liquid analyte shown in Fig. 4. The linear fitting equation is λ_{peak}=-8383.9n_{eff}+13591.4 (1.454≤n_{eff}≤1.478). The refractive index of liquid analyte ranges from 1.454 to 1.478 which makes the resonant wavelength blue shift from 1407 nm to 1205 nm. The sensor has an average sensitivity of -8383.9 nm/RIU (refractive index unit) and the R-square is 0.99621. Meanwhile, the full width at half maximum (FWHM) of loss spectrum decreases as the refractive index of liquid analyte increases. Figure of merit (FOM) is an important parameter to assess fiber sensors. The sensor has an average FOM of 168.16 RIU^{-1} (FOM=Sensitivity/FWHM). High sensitivity, good linearity, and nice FOM of the proposed sensor are distinctly promising for biochemical detection.

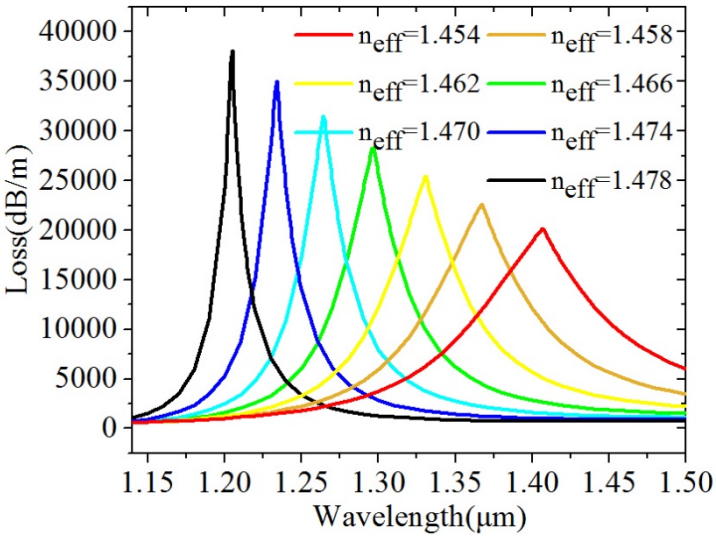

Fig. 3. The confinement loss of liquid-core mode in y-polarized direction at different refractive indices of liquid analyte as the plasma material is gold.

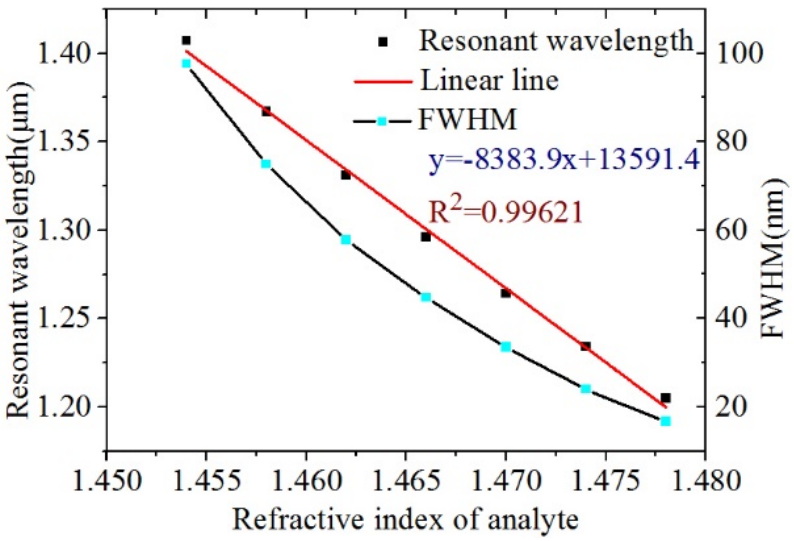

Fig. 4. Resonance wavelength and FWHM of the loss spectrum depending on the refractive index of liquid analyte.

3.1. Plasma material silver and aluminum

Obviously, one of the significant influences on the SPR-PCF sensor is the plasma material chosen to be filled. Therefore, we analyze the cases that the yellow holes are filled with silver and aluminum respectively. The structural parameters are D_1=1.8 μm, D_2=1.2 μm, D_3=2.0 μm, d=0.8 μm and Λ=2 μm. Fig. 5(a) shows the confinement loss at various refractive indices of liquid analyte from 1.454 to 1.478 as the plasma material is silver. It is easy to find that the loss spectrum of y-polarized mode is almost same as that by the PCF filled with gold wire. While the resonance wavelength red shifts slightly compared with the PCF filled with gold wire at the same refractive index of liquid analyte. The resonance wavelength blue shifts, the resonance loss increases and the FWHM becomes smaller as the refractive index of liquid analyte increases. We plot a fitting line between the resonance wavelength and the refractive index of liquid analyte shown in Fig. 5(b). Similarly, the linear fitting equation and the R-square are given. The fiber sensor based on PCF filled with silver wire possesses the sensitivity of -8428.6 nm/RIU and R-square of 0.99665. We find that the average sensitivity of the sensor based on PCF filled with silver is almost the same as that filled with gold wire as the refractive index of liquid analyte varies from 1.454 to 1.478. Silver is the ideal material due to its low optical damping and non-interband transitions, but it is easily oxidized to form a layer of silver oxide with

completely different properties that affects the performances and practicability of the fiber sensor.

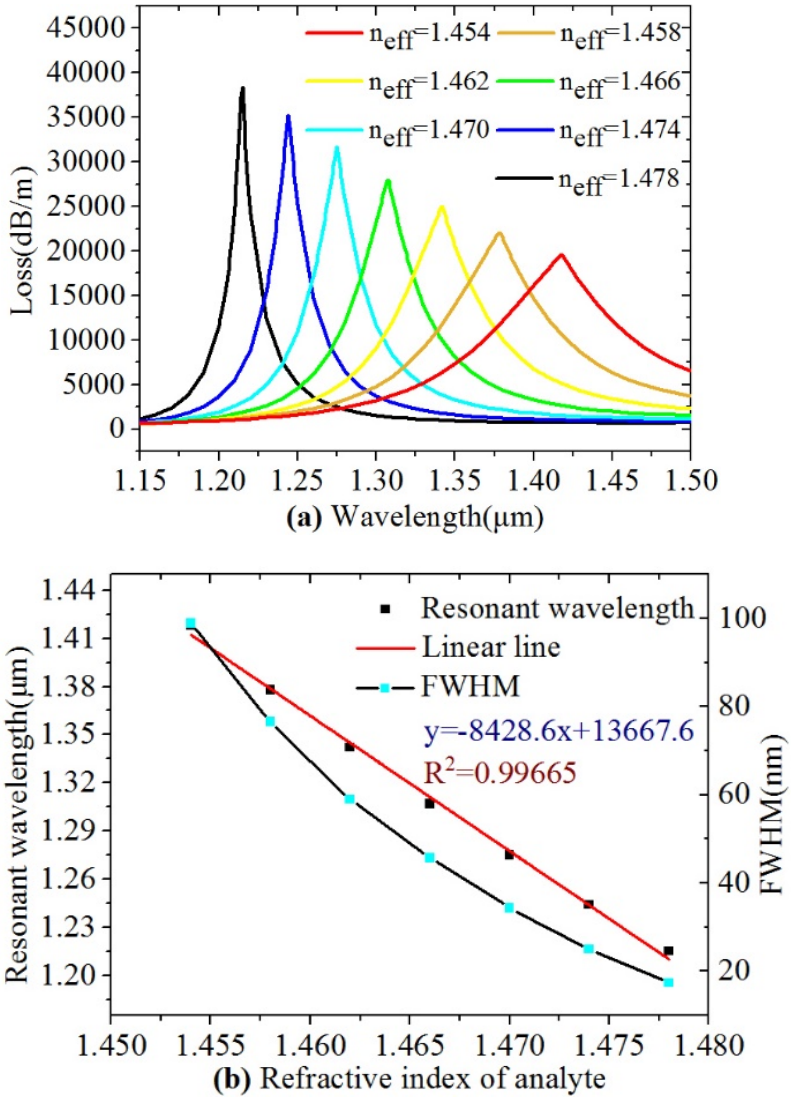

Fig. 5. (a) Wavelength-dependent confinement loss of y-polarized mode at different indices of liquid analyte. **(b)** The resonant wavelength and FWHM depending on the refractive index of liquid analyte. The plasma material is silver.

Next, we will change the plasma material into aluminum to be filled into the yellow holes of the PCF. The structural parameters of the PCF are D_1=1.8 μm, D_2=1.2 μm, D_3=2.0 μm, d=0.8 μm and Λ=2 μm. The loss spectra of the PCF filled with aluminum are shown in Fig. 6(a), the refractive index of liquid analyte varies from 1.454 to 1.478. We find the resonance wavelength blue shifts when the refractive index of liquid analyte increases. The loss firstly increases and then decreases which

is distinct from that filled with gold or silver wire. The mechanism behind this is unknown currently. The resonance wavelength blue shifts at the same refractive index of liquid analyte compared with that filled with gold or silver wire. Fig. 6(b) shows the resonance wavelength and FWHM depending on wavelength. The fiber sensor based on PCF filled with aluminum wire possesses the sensitivity of -8776.8 nm/RIU with the goodness of fit parameter R^2 of 0.99345. The FWHM also increases firstly and then decreases. The fiber sensor has a higher sensitivity compared with that based on PCF filled with gold or silver wire. Aluminum is aslo oxidized easily. The sensitivity of the fiber sensor with gold wire is lower than that with silver or aluminum wire, while the difference is small. Therefore, we choose gold wire as the plasma material to be filled into the structure of the PCF due to its stable physicochemical properties and better sensing performances in the biochemical sensing field.

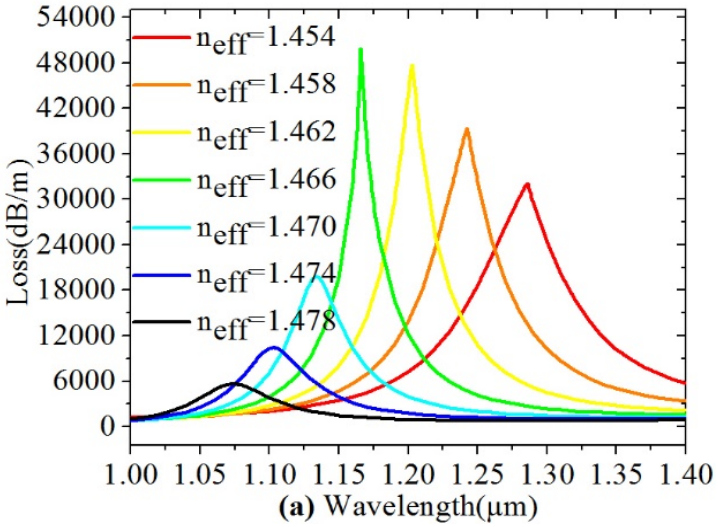

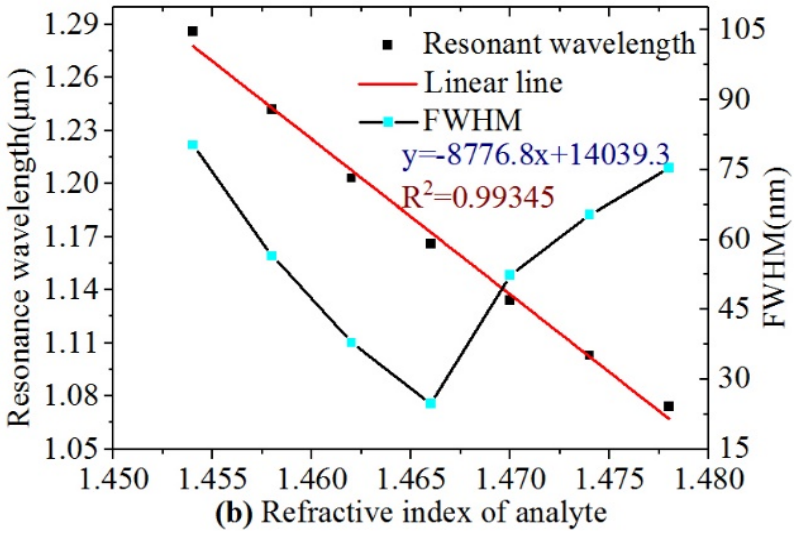

Fig. 6. (a) The loss spectrum of y-polarized mode at different refractive indices of liquid analyte. **(b)** The resonance wavelength and FWHM depending on the refractive index of liquid analyte. The plasma material is aluminum.

3.2. Adjustment of structural parameters

Generally, the performances of PCF can be readily modulated by changing the geometrical parameters of the PCF. The influences of structural parameters D_1, D_2 and D_3 on the sensing characteristics are analyzed in the following part when the refractive indices of liquid analyte are n_{eff}=1.458 and n_{eff}=1.470 respectively. The plasma material is gold. Fig. 7 shows the influences of the central hole diameter D_1 on the resonant wavelength and confinement loss when the other geometrical parameters D_2=1.2 μm, D_3=1.8 μm, d=0.8 μm and Λ=2.0 μm stay unchanged. It is easy to find that the confinement loss grows slightly and the resonant wavelength blue shifts at the same index of liquid analyte as the diameter D_1 increases. The FWHM can be decreased by increasing the diameter D_1 and the resolution can be improved. Meanwhile, increased confinement loss can improve sensing characteristics and prevents other factors from affecting the sensor. While the influence of structural parameter D_1 on the sensitivity of the proposed sensor are very weak.

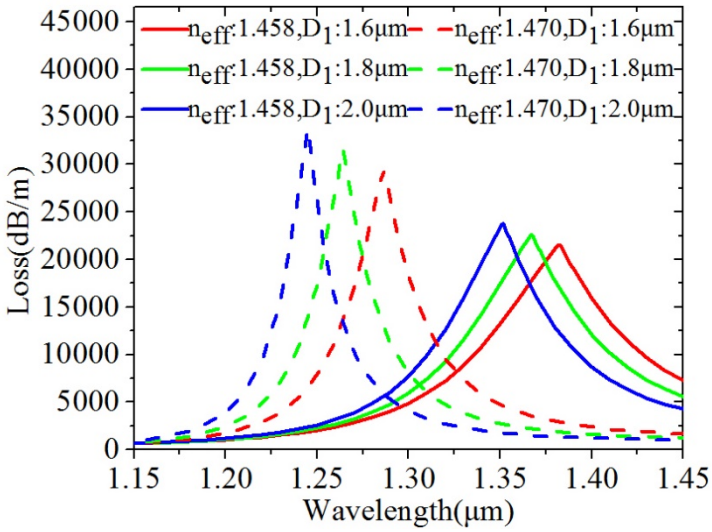

Fig. 7. The confinement loss depending on the controllable wavelength by varying the liquid-core hole diameter D_1 from 1.6 μm to 2.0 μm as the refractive indices of liquid analyte are 1.458 and 1.470, and the other structural parameters are D_2=1.2 μm, D_3=2.0 μm, d=0.8 μm and Λ=2.0 μm.

The diameter D_2 of gold wire also has some effects on the confinement loss and the resonance wavelength. The liquid core will gradually approach to the gold wire as the diameter D_2 of gold wire increases, which allows coupling between core mode and SPP mode become easier. The diameter D_2 of gold wire are 0.8 μm, 1.0 μm and 1.2 μm, and the other structural parameters are D_1=1.8 μm, D_3=2.0 μm, d=0.8 μm and Λ=2.0 μm. As it depicts in Fig. 8, the resonance loss decreases with the increment of diameter D_2 of gold wire as the refractive index of liquid analyte is 1.458. While the resonance loss is not changed regularly as the refractive index of liquid analyte is 1.470. Meanwhile, the resonant wavelength red shifts when the diameter D_2 of gold wire increases, which is due to that SPP mode has a higher refractive index and the index of liquid-core mode is nearly not changed. Noticeably, we can know that it has a blue shift for the resonant wavelength and the resonance loss rises on account of the increasing of the refractive index of liquid analyte from 1.458 to 1.470 except that the resonance loss decreases suddenly when n_{eff}=1.470 and D_2=0.8 μm. The FWHM becomes better with the diameter D_2 decreasing when the refractive index of liquid analyte is 1.458. While the FWHM is not changed regularly when the refractive index of liquid analyte is 1.470. We also find that the sensitivity is slightly increased with the diameter D_2 increasing.

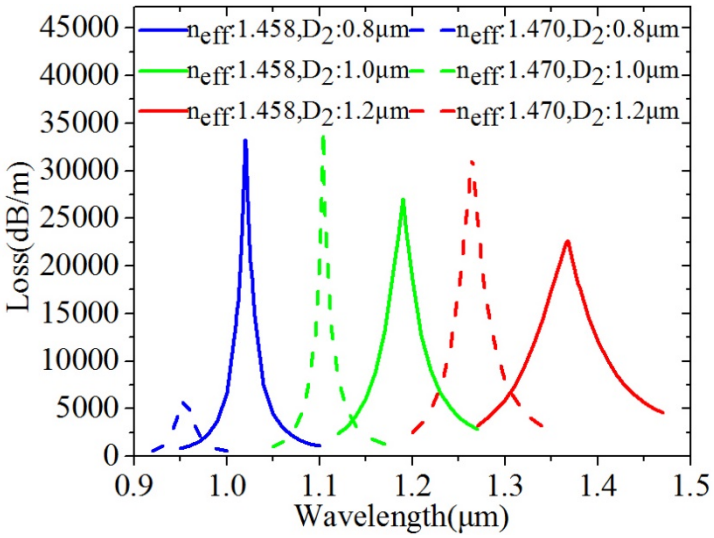

Fig. 8. The confinement loss depending on the wavelength for n_{eff}=1.458 and 1.470 by setting the diameter D_2 of gold wire as 0.8 μm, 1.0 μm and 1.2 μm, while the other structural parameters are D_1=1.8 μm, D_3=2.0 μm, d=0.8 μm and Λ=2.0 μm.

The effects of the diameter D_3 of the bigger air holes in the x direction on the resonance wavelength and confinement loss are analyzed and the loss spectra are shown in Fig. 9. D_3 are 1.6 μm, 1.8 μm and 2.0 μm respectively, the other structural parameters are D_1=1.8 μm, D_2=1.2 μm, d=0.8 μm and Λ=2.0 μm. The trend is observed that resonant wavelength moves to longer wavelength with the diameter D_3 increasing when the refractive index of liquid analyte is 1.458 or 1.470. Because the fiber-mode index decreases and the SPP-mode index remains unchanged nearly which results in the coupling point red shifting. The confinement loss shrinks at the same refractive index of liquid analyte because less energy is emitted into the cladding of the PCF due to the increase of the diameter D_3. Moreover, the sensitivity of the fiber sensor based on PCF becomes larger slightly and the FWHM becomes wider. We can also conclude that the sensitivity and FWHM increase with an increase in wavelength.

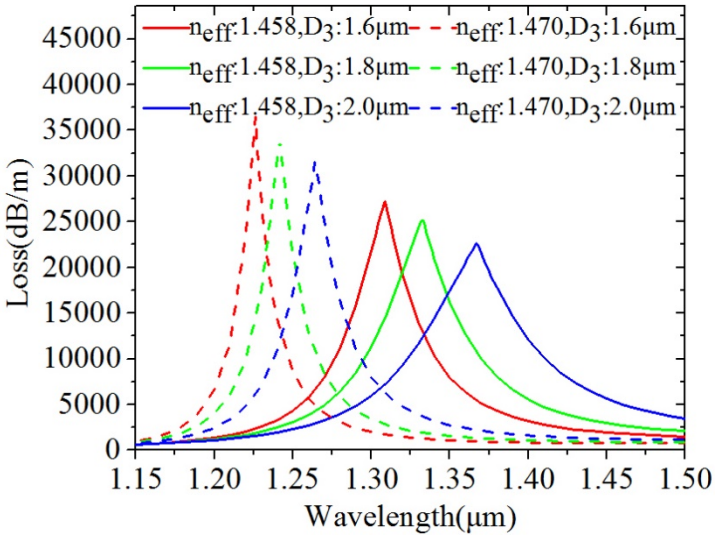

Fig. 9. Confinement loss depending on the wavelength for n_{eff}=1.458 and 1.470 as the diameter D_3 are 1.6 μm, 1.8 μm and 2.0 μm, while the other structural parameters are D_1=1.8 μm, D_2=1.2 μm, d=0.8 μm and Λ=2.0 μm.

6. Conclusion

A kind of liquid-core PCF biochemical sensor based on surface plasmon resonance has been presented in this paper. Liquid analyte to be measured is filled into the central hole of the PCF which supports liquid-core mode. Mode resonance appears as the liquid-core mode and SPP mode satisfy phase matching condition which can be used to detect analyte. The fiber sensor based on PCF filled with gold wire possesses the sensitivity of -8383.9 nm/RIU, FOM of 168.16 RIU^{-1} and R-square of 0.99621. The sensitivities are up to -8428.6 nm/RIU and -8776.8 nm/RIU by filling silver and aluminum respectively into the air holes of the PCF which are a little higher than the sensitivity by filling gold into the PCF. The structural parameters of D_1, D_2 and D_3 have a little impact on the sensing characteristics of the PCF showing that the fiber sensor possesses good stability.

Acknowledgement

This research was funded by the National Natural Science Foundation of China (Grant No. 51907017), Key Science and Technology Research Projects of Higher Education Institutions in Hebei Province of China (Grant No. ZD2019304), Fundamental Research Funds for the Central Universities of China (Grant No. N182304011) and

China National Fund for Studying Abroad. The authors thank Christopher Markwell of Northumbria University for his revision in language.

References

[1] P. Russell, Photonic crystal fibers, Science 299(5605) 2003 358-362.

[2] X. Yu, Y. Sun, G.B. Ren, et al., Evanescent field absorption sensor using a pure-silica defected-core photonic crystal fiber, IEEE Photon. Technol. Lett. 20(5) 2008 336-338.

[3] B. Fu, S. Li, Y. Yao, et al. Improved high birefringence photonic crystal fibres with dispersion flattened and single mode operation, Chinese Phys. B. 20(2) 2011 024209.

[4] B. Fu, S. Li, Y. Yao, et al., Coupling characteristics of dual-core high birefringence photonic crystal fibers, Acta Phys. Sin-Ch. Ed 58(11) 2009 7708-7715.

[5] M. Wang, F. Wang, S. Feng, et al., 272 W quasi-single-mode picosecond pulse laser of ytterbium-doped large-mode-area photonic crystal fiber, Chin. Opt. Lett. 17(7) 2019 071401.

[6] F. Tani, F. Köttig, D. Novoa, et al., Effect of anti-crossings with cladding resonances on ultrafast nonlinear dynamics in gas-filled photonic crystal fibers, Photonics Res. 6(2) 2018 84-88.

[7] Y. Tao, and S.P. Chen, All-fiber high-power linearly polarized supercontinuum generation from polarization-maintaining photonic crystal fibers, High Power Laser Sci. 7 2019 e28.

[8] Q. Liu, S. Li, and X.Y. Wang, Sensing characteristics of a MF-filled photonic crystal fiber Sagnac interferometer for magnetic field detecting, Sensor. Actuat. B-Chem. 242 2017 949-955.

[9] Q. Liu, L. Xing, S.C. Yan, et al., Sensing characteristics of photonic crystal fiber sagnac interferometer based on novel birefringence and Vernier effect, Metrologia 2020 https://doi.org/10.1088/1681-7575/ab71b2.

[10] X. Li, L. Nguyen, M. Becker, et al., Simultaneous measurement of temperature and refractive index using an exposed core microstructured optical fiber, IEEE J. Quantum Elect. 26(4) 2019 1-7.

[11] R.H. Ritchie, Plasma losses by fast electrons in thin films, Phys. Rev. 106(5) 1957 874.

[12] M.B. Hossain, M.S. Hossain, M. Moznuzzaman, et al., Numerical analysis and design of photonic crystal fiber based surface plasmon resonance biosensor, J. Sens. Technol. 9(2) 2019 27-34.

[13] E. Haque, S. Mahmuda, M.A. Hossain, et al., Highly sensitive dual-core PCF based plasmonic refractive index sensor for low refractive index detection, IEEE Photon. J.11(5) 2019 1-9.

[14] Y. Zhao, R.J. Tong, F. Xia, et al., Current status of optical fiber biosensor based on

surface plasmon resonance, Biosens. Bioelectron. 142 2019 111505.

[15] H.W. Lee, M.A. Schmidt, R.F. Russell, et al., Pressure-assisted melt-filling and optical characterization of Au nano-wires in microstructured fibers, Opt. Express 19(13) 2011 12180-12189.

[16] S. Zhang, X. Yu, Y. Zhang, et al., Theoretical study of dual-core photonic crystal fibers with metal wire, IEEE photon. J. 4(4) 2012 1178-1187.

[17] M.R. Hasan, S. Akter, K. Ahmed, et al., Plasmonic refractive index sensor employing niobium nanofilm on photonic crystal fiber, IEEE Photon. Technol. Lett. 30(4) 2017 315-318.

[18] A.A. Rifat, G.A. Mahdiraji, R. Ahmed, et al., Copper-graphene-based photonic crystal fiber plasmonic biosensor, IEEE Photon. J. 8(1) 2015 1-8.

[19] Z. Fan, S. Li, Q. Liu, et al., High sesitivity of refractive index sensor based on analyte-filled photonic crystal fiber with surface plasmon resonance, IEEE Photon. J. 7(3) 2015 1-9.

[20] Z. Guo, Z. Fan, X. Kong, et al., Photonic crystal fiber based wide-range of refractive index sensor with phase matching between core mode and metal defect mode, Opt. Commun. 461 2020 125233.

[21] T. Li, L. Zhu, X. Yang, et al., A refractive index sensor based on H-shaped photonic crystal fibers coated with Ag-graphene layers, Sensors 20(3) 2020 741.

[22] Y. Liu, S. Li, H. Chen, et al., Surface plasmon resonance induced high sensitivity temperature and refractive index sensor based on evanescent field enhanced photonic crystal fiber, J. Lightw. Technol. 2019. 10.1109/JLT.2019.2949067

[23] C. Liu, W. Su, Q. Liu, et al., Symmetrical dual D-shape photonic crystal fibers for surface plasmon resonance sensing, Opt. Express 26(7) 2018 9039-9049.

[24] F. Zha, J. Li, P. Sun, et al., Highly sensitive selectively coated D-shape photonic crystal fibers for surface plasmon resonance sensing, Phys. Lett. A 383(15) 2019 1825-1830.

[25] A.A. Rifat, R. Ahmed, G.A. Mahdiraji, et al., Highly sensitive D-shaped photonic crystal fiber-based plasmonic biosensor in visible to near-IR, IEEE Sens. J. 17(9) 2017 2776-2783.

[26] Q. Liu, B. Yan, and J. Liu, U-shaped photonic quasi-crystal fiber sensor with high sensitivity based on surface plasmon resonance, Appl. Phys. Express 12(5) 2019 052014.

[27] T. Wu, Y. Shao, Y. Wang, et al., Surface plasmon resonance biosensor based on gold-coated side-polished hexagonal structure photonic crystal fiber, Opt. Express 25(17) 2017 20313-20322.

[28] X. Xin, S. Li, T. Cheng, et al., Numerical simulation of surface plasmon resonance based on Au-metalized nanowires in the liquid-core photonic crystal fibers, Optik 126(15-16) 2015 1457-1461.

[29] N. Chen, M. Chang, X. Lu, et al., Photonic crystal fiber plasmonic sensor based on dual

optofluidic channel, Sensors 19(23) 2019 5150.

[30] G. Ghosh, M. Endo, and T. Iwasaki, Temperature-dependent Sellmeier coefficients and chromatic dispersions for some optical fiber glasses, J. Lightw. Technol. 12(8) 1994 1338-1342.

[31] A. Vial, A.S. Grimault, D. Macías, et al., Improved analytical fit of gold dispersion: Application to the modeling of extinction spectra with a finite-difference time-domain method, Phys. Rev. B 71(8) 2005 085416.

[32] A.D. Rakić, A.B. Djurišić, J.M. Elazar, et al., Optical properties of metallic films for vertical-cavity optoelectronic devices, Appl. Optics 37(22) 1998 5271-5283.

[33] Y. Wang, C.R. Liao, and D.N. Wang, Femtosecond laser-assisted selective infiltration of microstructured optical fibers, Opt. Express 18(17) 2010 18056-18060.

[34] Q. Liu, S. Li, and H. Chen, Two kinds of polarization filter based on photonic crystal fiber with nanoscale gold film, IEEE Photon. J. 7(1) 2015 1-11.